A novel 2-oxoindolinylidene inhibitor of bacterial MurD ligase: Enzyme kinetics, protein-inhibitor binding by NMR and a molecular dynamics study

ARTICLE *in* EUROPEAN JOURNAL OF MEDICINAL CHEMISTRY · JUNE 2014

Impact Factor: 3.45 · DOI: 10.1016/j.ejmech.2014.06.021 · Source: PubMed

6 AUTHORS, INCLUDING:

Mihael Simcic

EN-FIST Centre of Excellence

9 PUBLICATIONS **104** CITATIONS

SEE PROFILE

Katja Kristan

University of Ljubljana

28 PUBLICATIONS **294** CITATIONS

SEE PROFILE

Darko Kocjan

National Institute of Chemistry

50 PUBLICATIONS **376** CITATIONS

SEE PROFILE

Simona Golič Grdadolnik

National Institute of Chemistry

110 PUBLICATIONS **1,313** CITATIONS

SEE PROFILE

European Journal of Medicinal Chemistry 83 (2014) 92–101

Contents lists available at ScienceDirect

European Journal of Medicinal Chemistry

journal homepage: http://www.elsevier.com/locate/ejmech

Original article

A novel 2-oxoindolinylidene inhibitor of bacterial MurD ligase: Enzyme kinetics, protein-inhibitor binding by NMR and a molecular dynamics study

Mihael Simčič [a, b, 1], Kaja Pureber [a, b], Katja Kristan [c], Uroš Urleb [c, 2], Darko Kocjan [a, b, *], Simona Golič Grdadolnik [a, b, **]

[a] EN-FIST Centre of Excellence, Dunajska 156, 1000 Ljubljana, Slovenia
[b] Laboratory of Biomolecular Structure, National Institute of Chemistry, Hajdrihova 19, 1001 Ljubljana, Slovenia
[c] Sandoz Development Centre Slovenia, Lek Pharmaceuticals, Verovškova 57, 1526 Ljubljana, Slovenia

ARTICLE INFO

Article history:
Received 28 November 2013
Received in revised form
30 May 2014
Accepted 10 June 2014
Available online 11 June 2014

Keywords:
MurD ligase
2-Oxoindolinylidene inhibitor
Steady-state enzyme kinetics
NMR
Molecular dynamics

ABSTRACT

N-(5-(5-nitro-2-oxo-1,2-dihydro-3H-indol-3-ylidene)4-oxo-2-thioxo-1,3-thiazolidin-3-yl)nicotinamide, a 2-oxoindolinylidene derivative with novel structure scaffold, was evaluated for inhibition potency against the MurD enzyme from *Escherichia coli* using an enzyme steady-state kinetics study. The compound exerted competitive inhibition with respect to UMA, a MurD substrate, and affected bacterial growth. Furthermore, we isolated and purified ^{13}C selectively labeled MurD enzyme from *E. coli* and evaluated the binding interactions of the new compound using the $^{1}H/^{13}C$-HSQC 2D NMR method. Molecular dynamics calculations showed stable structure for the MurD-inhibitor complex. The binding mode of novel inhibitor was determined and compared to naphthalene-*N*-sulfonamide-D-Glu derivatives, transition state mimicking inhibitors, UMA and AMP-PCP, an ATP analog. It binds to the UDP/MurNAc binding region. In contrast to transition state mimicking inhibitors, it does not interact with the enzyme's *C*-terminal domain, which can be beneficial for ligand binding. A pharmacophore pattern was established for the design of novel drugs having a propensity to inhibit a broad spectrum of Mur enzymes.

1. Introduction

The bacterial enzyme UDP-*N*-acetylmuramyl-L-alanine:D-glutamate ligase (MurD) belongs to a family of Mur ligases that are essential for the synthesis of bacterial peptidoglycan. Mur ligases C to F synthesize the main building peptidoglycan element, the UDP-muramyl pentapeptide, by successively adding L-Ala, D-Glu, *meso*-2,6 diaminopimelic acid and dipeptide D-Ala-D-Ala. Mur ligases represent an attractive target, potentially useful for the discovery of new antibacterial agents.

MurD catalyzes the formation of the peptide bond between UDP-MurNAc-L-Ala substrate (UMA) and D-Glutamic acid. In the first stage, the terminal carboxyl group of UMA substrate is phosphorylated by ATP. Resulting acylphosphate intermediate is then attacked by the amine group of the incoming D-Glu. High energy tetrahedral intermediate is formed, which then yields product UDP-*N*-acetylmuramyl-L-alanine (UMAG) and inorganic phosphate.

MurD comprises three structural domains: an *N*-terminal domain responsible for the binding of the UDP moiety of UMA, a

Abbreviations: MurD, UDP-N-acetylmuramyl-L-alanine:D-glutamate ligase; UMA, UDP-N-acetylmuramyl-L-alanine; UMAG, UDP-N-acetylmuramyl-L-alanine-D-glutamate; AMP-PCP, adenylyl 5′-(β,γ-methylene)diphosphonate; MD, molecular dynamics; MIC, minimal inhibitory concentrations; HSQC, heteronuclear single quantum coherence; CSP, chemical shift perturbations; STD, saturation transfer difference; NOESY, nuclear Overhauser effect correlation spectroscopy; CLSI, Clinical and Laboratory Standards Institute.

* Corresponding author. EN-FIST Centre of Excellence, Dunajska 156, 1000 Ljubljana, Slovenia.
** Corresponding author. Laboratory of Biomolecular Structure, National Institute of Chemistry, Hajdrihova 19, 1001 Ljubljana, Slovenia.
E-mail addresses: darko.kocjan@ki.si (D. Kocjan), simona.grdadolnik@ki.si (S.G. Grdadolnik).
[1] Present address: EN-FIST Centre of Excellence, Dunajska 156, 1000 Ljubljana, Slovenia.
[2] Present address: Sandoz International, Global Product Development, 83607 Holzkirchen, Germany.

http://dx.doi.org/10.1016/j.ejmech.2014.06.021
0223-5234/

central ATP-binding domain and a *C*-terminal domain involved in the binding of the amino acid substrate D-Glu [1]. The binding interactions of the substrate UMA and the product ADP are known from the X-ray structures of the complexes of MurD with UMA and ADP [1,2].

Several groups of MurD inhibitors are reported in the literature. The first potent inhibitors designed were phosphinate inhibitors [3,4]. These compounds were highly valuable for the study of the enzyme's structure and its kinetics. Later, a series of naphthalene-*N*-sulfonyl-D-glutamic acid inhibitors were synthesized [5,6] that mimic the transition-state, tetrahedral intermediate. Inhibitors from this series were the first compounds for which the crystal structure in complex with MurD enzyme was revealed [5]. The first generation of sulfonamide inhibitors was followed by the second generation, which featured rigid D-glutamic acid analogs [7]. The substitution of the flexible D-glutamic acid with rigid mimetics resulted in significantly improved inhibitory activities compared to the first generation of sulfonamide inhibitors. Both generations of sulfonamide inhibitors share a similar binding mode where D-Glutamic acid (or rigid D-Glutamic acid analog) occupies the D-Glu binding site in the *C*-terminal domain, the other end of the inhibitor occupies the hydrophobic uracil binding pocket in the *N*-terminal domain and the middle part of the molecule interacts with the central domain [6-9].

In previous studies, we performed extensive NMR and molecular dynamic studies of both generations of sulfonamide inhibitors in complex with MurD [8,9] that revealed a new aspect for the rational design of potent Mur ligase inhibitors. Complex dynamic behavior of these ligand-MurD complexes was observed. The ligand-MurD interactions are affected by movements of the protein domains and by the flexibility of the ligand. The interference of ligand-MurD interactions between different domains was observed, which prevents an optimal fitting of particular binding regions and exerts conformational flexibility on the bound ligands. Both generations of sulfonamide inhibitors are significantly affected by the protein domain motions, because they span from the *C*-terminal domain to the *N*-terminal domain and also interact with the central domain.

Failures in the design of highly potent transition state analogs can be attributed to the ignorance of dynamic processes in ligand-MurD complexes. The dynamic aspect of ligand binding can also explain the comparable inhibitory activities of inhibitors that interact with different number of MurD domains. For example, NMR studies have shown that hydroxy substituted 5-benzelidenethiazolidin-4-one inhibitors interact only with the uracil binding pocket (*N*-terminal domain), while 2-thioxothiazolidin-4-one inhibitors interact only with the D-Glu binding site (*C*-terminal domain) and central domain. However, the activities of the most potent derivatives of these two types of MurD inhibitors are similar to the most potent derivatives of the second generation of sulfonamide inhibitors or to the most potent derivatives of other types of transition state analogs like 5-benzylidenerhodanine and 5-benzelidenethiazolidine-2,4-dione inhibitors [10–12], which interact with all three MurD domains.

Generally, the great majority of the MurD inhibitors with the known mechanism of action lack antibacterial activity [13]. Weak antibacterial activity was observed only for the hydroxy substituted 5-benzelidenethiazolidin-4-one derivative [14] and for some 5-benzylidenerhodanine derivatives [12].

The identification of inhibitors with novel structure scaffolds can be a very useful in order to gain a better insight into the structural requirements for effective inhibition of MurD together with antibacterial activity. A 2-oxoindolinylidene derivative (Fig. 1) was discovered by virtual screening of commercially available compound databases at Lek Pharmaceuticals, a Sandoz Company, and demonstrated that it possessed promising inhibitory activity against the MurD enzyme.

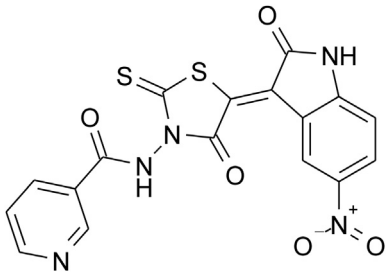

Fig. 1. Structure of *N*-(5-(5-nitro-2-oxo-1,2-dihydro-3H-indol-3-ylidene)-4-oxo-2-thioxo-1,3-thiazolidin-3-yl)nicotinamide (compound **1**).

In this study, the inhibition constant of compound **1** for the MurD enzyme from *Escherichia coli* was evaluated. Additionally, compound **1** was assayed *in vitro* for its antibacterial activity against several Gram-positive and Gram-negative bacterial strains. We focused on the determination of the binding mode of compound **1** to the MurD enzyme at the atomic level using NMR methods. The $^{1}H/^{13}C$ chemical shift perturbations (CSP) in MurD selectively labeled with ^{13}C at the methyl groups of Ile, Val and Leu [15] upon binding of compound **1** were examined and its binding mode was analyzed in relation to UMA, AMP-PCP and some of the naphthalene *N*-sulfonamide-D-Glu inhibitors elaborated earlier. Using molecular dynamics (MD) simulations, we verified the specific action of compound **1** and evaluated the role of the structural fragments, nicotinamide, 4-oxo-2-thioxo-1,3-thiazolidine and 5-nitro-2-indolone, connected rigidly by a double bond, in interactions with the MurD binding site.

The results show the interaction profile of a novel structure scaffold of compound **1**, which provided a pharmacophore pattern and gave some useful conclusions to help direct the design of Mur inhibitors. Compound **1** is located in the region of the UMA binding site occupied by the uridine and the MurNAc moieties. All MurA-G enzymes share identical UDP and similar GlcNAc/MurNAc substrate moieties. Therefore, inhibitors designed to mimic the UDP-GlcNAc/UDP-MurNAc part of substrates could potentially lead to inhibition of a very broad spectrum of Mur enzymes. This binding region of MurD has been so far underexploited, since the majority of known MurD inhibitors do not extend into the MurNAc binding region. Another significant point for the design of optimized inhibitors using the determined binding mode of compound **1** is related to the position of compound **1** with respect to the three domains of the MurD enzyme. Compound **1** interacts only with the residues of the *N*-terminal and central domains. According to our NMR studies of various types of MurD inhibitors, with different binding modes, we believe that the interaction with a reduced number of domains can be beneficial for ligand binding. The interference of ligand-MurD interactions between the *N*- and *C*-terminal domains is especially critical for ligand binding [9].

2. Results and discussion

2.1. Biological activity

Steady-state enzyme kinetic analysis was performed by application of a slightly modified malachite green assay. The utility of the assay for inhibitor characterization was evaluated by the determination of the kinetic parameter $K_{M,app}$ for each *E. coli* MurD substrate. Fig. S1A–C in supporting information show the saturation plot and the corresponding Lineweaver–Burk plot for each substrate. The apparent K_M values determined (ATP: 97 ± 9 μM, UMA:

7 ± 0.6 μM, D-Glu: 42 ± 5 μM) are close to the previously measured ones [5,16]. Kinetic studies were performed to determine the type of inhibition for compound **1**. The results presented in Fig. S1D in supporting information show the best fits, as judged by the R^2 value, where compound **1** is seen to be a competitive inhibitor with a K_I value of 115 ± 18 μM with respect to UMA.

Compound **1** was assayed *in vitro* for its antibacterial activity against several standard Gram-positive and Gram-negative bacterial strains using the macrodilution method in accordance with the standard reference recommendations of the CLSI (Clinical and Laboratory Standards Institute). It showed weak antibacterial activities against Gram-negative *Haemophilus influenzae* (ATCC 49247) and Gram-positive *Enterococcus faecalis* (ATCC 29212) bacterial strains with a minimal inhibitory concentration (MIC) of 128 μg/mL (Supporting information, Table S1).

2.2. NMR studies of ligand binding

The specific binding of compound **1** was studied by application of saturation transfer difference (STD), transferred NOESY and $^1H/^{13}C$-HSQC 2D NMR spectroscopy. The results of the STD and transferred NOESY experiments demonstrate that all proton rich segments of inhibitor **1** are in contact with the MurD receptor (Supporting information, Chart S1).

Monitoring of the $^1H/^{13}C$ CSP of MurD selectively labeled with ^{13}C at the methyl groups of Ile (δ1 only), Val and Leu [15] upon raising the inhibitor molar ratio was used to determine the dissociation constant (K_D), the binding site and the inhibitor's location.

The signals that clearly exhibit fast motion exchange without line broadening effects [17] were selected to determine the K_D. The combined $^1H/^{13}C$ CSP data were fitted to the one-site binding model. The titration curves that gave an average K_D value of 98 ± 17 μM are presented (Fig. 2; Supporting information, Table S2).

The combined $^1H/^{13}C$ CSP of the new inhibitor were compared to those of UMA, AMP-PCP and naphthalene-*N*-sulfonyl-D-Glu derivatives **2** and **3** (Fig. 3). The combined CSP calculated from the ^1H and ^{13}C chemical shifts in the absence and presence of the ligands at 5:1 ligand:MurD ratio are presented in Fig. 4. Full $^1H/^{13}C$-HSQC spectrum with peak numbering, the corresponding list of chemical shifts and the overlay of $^1H/^{13}C$-HSQC in presence and absence of compound **1** are available in supporting information (Figs. S2, S3 and Table S3).

Assignments of crucial Ile74, Leu57 and Leu416 methyl groups in the MurD binding site that indicate binding to the uracil (Ile74, Leu57) or to the D-Glu (Leu416) binding sites were proposed in our recently published study of the binding mode of the second generation of sulfonamide derivatives [9]. These groups are in significantly closer spatial proximity to the bound naphthalene-*N*-sulfonyl-D-Glu derivatives compared to the rest of the labeled methyl groups. Therefore, the comparison of the MurD CSP patterns induced by the binding of different types of MurD ligands, published binding modes of these types of ligands as determined by X ray [2,5–7] or NMR studies [8,9,14,18] and theoretically predicted proton chemical shifts enabled their assignment [9]. The complete assignment of the methyl resonances was not preformed because of the insufficient stability of 47.7 kDa MurD and very low yields for the expression of the deuterated protein, which would be required for NMR assignment.

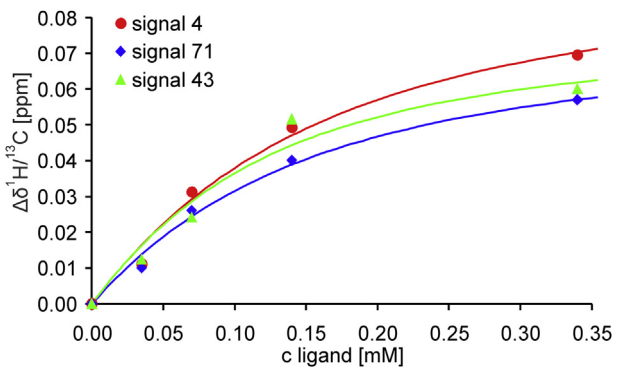

Fig. 2. The combined $^1H/^{13}C$ CSP (Δδ) of selected MurD methyl groups as a function of the concentration of compound **1** used to determine K_D.

In this study, we can propose also the assignment of Ile95 methyl group because the available crystal structures of MurD enzyme in complex with UMA substrate [2] indicate that the Ile74 and Ile95 methyl groups are in significantly closer spatial proximity to UMA than the rest of Ile methyl groups (Supporting information, Chart S2). Only two signals in the Ile region of $^1H/^{13}C$-HSQC (Fig. 4) have significantly larger CSP at binding of UMA. The signal assigned to Ile95 methyl group is not affected at binding of naphthalene-*N*-sulfonyl-D-Glu derivatives. That can be explained by the different location of UMA phosphate groups and its *N*-acetylmuramic acid ring compared to naphthalene-*N*-sulfonyl-D-Glu derivatives (Fig. 5; Supporting information, Chart S2).

The CSP pattern of MurD methyl groups upon binding of compound **1** clearly indicates its location in the UMA binding site (Fig. 4). Its effect is limited to the signals that are also affected by the binding of UMA. The most pronounced CSP upon binding of compound **1** are observed for the signals of Leu57 methyl groups, indicating its interaction with the uracil binding pocket (Figs. 4 and 6). The rest of the molecule is mainly located in the part of the binding site occupied by the UMA phosphate groups and *N*-acetylmuramic acid ring and does not interact with the *C*-terminal domain (D-Glu binding site). This conclusion is based on the fact that compound **1** does not affect the signals of Leu416 methyl groups. In addition, some methyl resonances are influenced only by the binding of UMA and compound **1** but not by the binding of naphthalene-*N*-sulfonyl-D-Glu derivatives.

2.3. Molecular dynamics at the receptor level

The binding interactions of the new inhibitor were further investigated by MD simulations at the receptor level. NMR experimental data and steady-state enzyme kinetic analysis indicate that compound **1** is located in the same binding pocket as UMA substrate. We expected that the 4-oxo-2-thioxo-1,3-thiazolidine ring occupies the location of UMA phosphate groups. As pointed out elsewhere, 4-oxo-2-thioxo-1,3-thiazolidine is considered a diphosphate mimetic [2,19]. The uracil binding pocket could be occupied either by nitroindole ring or by pyridine ring. Several structures of the inhibitor-MurD complex were generated by restrained minimization considering the possible relevant orientations of compound **1** in the binding site. Using different groups of hydrogen bonding restraints, the possibility of the formation of a similar hydrogen-bonding pattern as observed for bound UMA was investigated. In the next step, unrestrained minimization was performed. Resulting structures revealed four possible binding modes of compound **1** that were in agreement with experimental data. None of these binding modes exhibited the hydrogen bonding network of bound UMA substrate. Four structures representing these binding modes were selected for unrestrained MD simulations (Supporting information, Fig. S4). In the first selected structure, the pyridine ring is located in a similar position as the UMA phosphate group, close to the Leu15. In the second and the third structure, the pyridine ring occupies a similar position as the UMA sugar moiety close to the Gln162. The third structure differs from

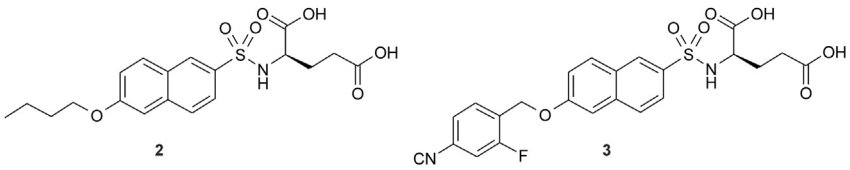

Fig. 3. Structure of *N*-(6-butoxy-naphthalene-2-sulfonamido)-D-glutamic acid (compound **2**) and *N*-(6-(4-Cyano-2-fluorobenzyloxy)naphthalene-2-sulfonamido)-D-glutamic acid (compound **3**).

the second in the orientation of the amide bond with respect to the 4-oxo-2-thioxo-1,3-thiazolidine ring. The fourth structure has pyridine ring located in the uracil binding pocket.

The MD trajectories revealed that during the simulation started with structure 3, compound **1** was the most stable compound in the proposed binding site. Very little ligand conformational flexibility was observed. Dihedral angles show almost no rotations (Supporting information, Fig. S5). In the other two trajectories, starting from structure 1 and 2, the pyridine ring was more flexible and exhibited fewer interactions. Additionally, stable hydrogen bonds were formed only in the third trajectory. The inhibitor was displaced from proposed binding site in the trajectory started from structure 4. Regarding the STD NMR data (Supporting information, Chart S1), which indicate interactions of all proton rich ligand segments with the binding site and comparable stability of the pyridine and 2-oxoindolinylidene rings, we concluded that the third trajectory is the most probable in terms of representing the binding mode of compound **1**.

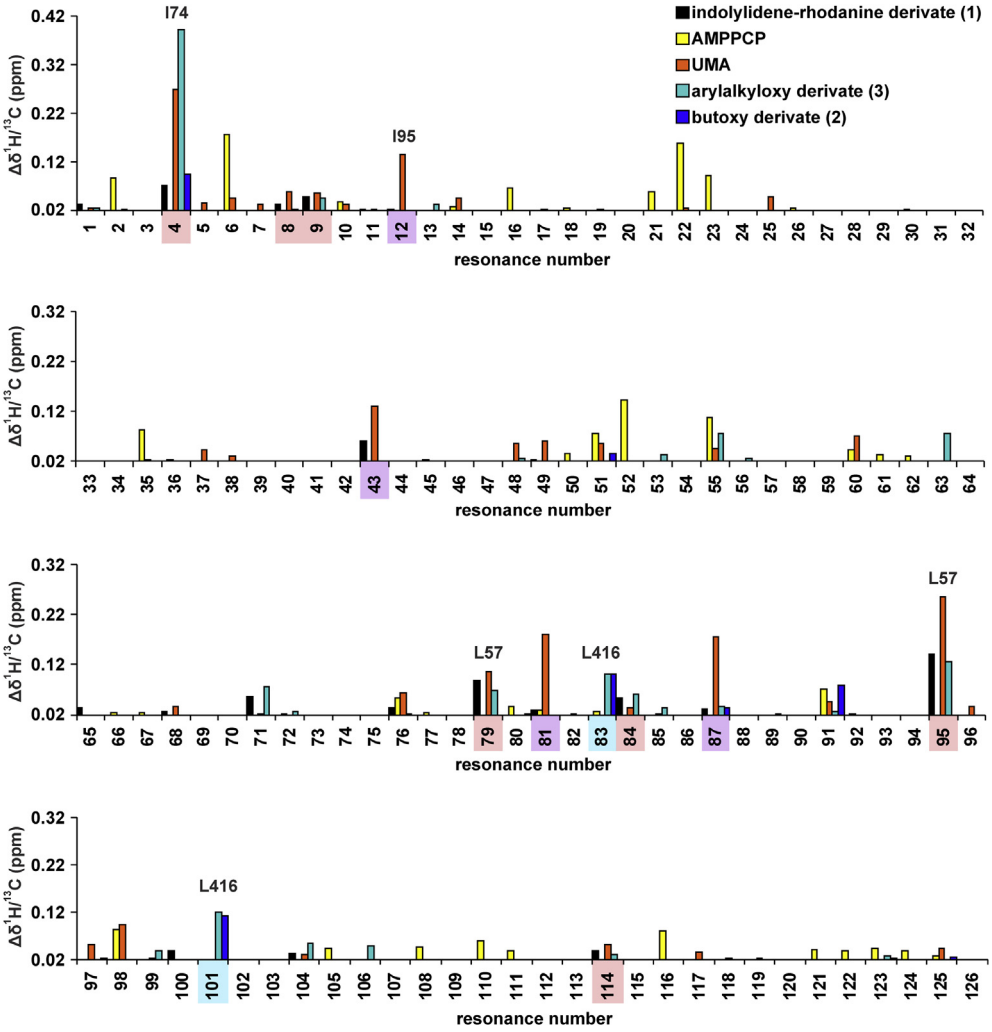

Fig. 4. Maps of combined $^{1}H/^{13}C$ CSP ($\Delta\delta$) of Ile (δ1 only), Val and Leu methyl groups of MurD upon binding of the ligands **1** (black), AMP-PCP (yellow), UMA (orange), compound **3** (cyan) and compound **2** (blue). The numbers of CSP characteristic for the binding in the uracil binding pocket, D-Glu binding site and UMA phosphate/muramyl binding region are highlighted with red, blue and purple boxes respectively. The proposed assignments of the methyl group signals in closest spatial proximity to the ligands are given. The threshold of 0.02 ppm was selected to neglect the effect of the 2% variation in DMSO-d_6 concentration on CSP. Only the sufficiently resolved resonances are included. The minimum possible CSP is presented for signals 83 and 101 (Leu416), since the signals move to the overlapped region of the spectra at a 1:1 and 5:1 ligand:MurD ratio respectively. Note that the numbering of CSP does not correspond to the MurD residue numbers but to the numbering of the resonances in the $^{1}H/^{13}C$-HSQC spectra. (For interpretation of the references to color in this figure legend, the reader is referred to the web version of this article.)

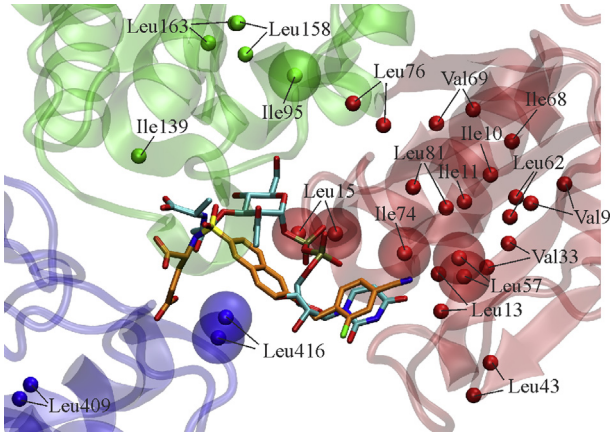

Fig. 5. Comparison of the binding modes of UMA (cyan) with arylalkyloxy derivative **3** (orange) in the MurD binding site as determined by X-ray diffraction [2,6]. The small red, blue and green spheres indicate Ile (δ1), Val and Leu methyl groups near the uracil-binding pocket, near the D-Glu-binding site and near the cleft-forming region of the central domain respectively. Methyl groups in the range of 5 Å are highlighted as larger transparent spheres. *N*-terminal, central and *C*-terminal domains are represented in red, green and blue respectively. (For interpretation of the references to color in this figure legend, the reader is referred to the web version of this article.)

The third trajectory revealed that compound **1** forms hydrogen bonds to different residues than UMA, despite its similar position in the UMA binding site (Fig. 7, Supporting information, Fig. S7). Stable hydrogen bond is formed between the pyridine nitrogen and the hydroxyl group of Ser159 (87% of the time). In addition, unstable but frequently formed hydrogen bonds are observed between the ligand amide oxygen and guanidine group of Arg186 (23% of the time) and between the ligand nitro group and hydroxyl group of Ser71 (27% of the time). Despite much less hydrogen bonding than in the case of the UMA substrate, compound **1** was firmly anchored in the proposed binding mode for all 20 ns of simulation. The very stable position of the 2-oxoindolinylidene ring in the uracil binding pocket was observed. This again points to the importance of hydrophobic interactions with the uracil binding pocket. Additionally, the 2-oxoindolinylidene ring forms a very stable π–π interaction with the Asp35–Arg37 salt bridge and a cation–π interaction with the charged guanidine group of Arg37. The 4-oxo-2-thioxo-1,3-thiazolidine ring has electrostatic interactions with the Gly73 amide and the Arg186 guanidine group. Additionally, weaker electrostatic interactions between the 4-oxo-2-thioxo-1,3-thiazolidine oxygen and the hydroxyl groups of Thr16 and Ser71 are present. The pyridine ring is close to Phe161, so π–π interaction is possible.

NMR experiments and MD simulations provided us with a scheme of binding interactions of inhibitor **1** with MurD residues (Fig. 8), as well as with some guidelines to design its derivatives with improved binding. MD analysis of binding energy contributions (Fig. 9) due to the molecular fragments, shows that the 2-oxoindolinylidene ring represents an essential part of compound **1**. Hydrophobic interactions with Ile11, Gly12, Gly73 and Ile74 in the uracil binding pocket and π–π interactions with salt-bridge Asp35–Arg37 are crucial. The nitro group also contributes to the binding in the uracil binding pocket. The keto oxygen and NH group do not seem to play essential roles in binding and may be omitted or modified. The 4-oxo-2-thioxo-1,3-thiazolidine ring does not have optimal interactions. It fails to mimic the phosphate groups of UMA, which have much better interactions. It seems to be the weakest part of the molecule as it has only medium range electrostatic interactions. The oxygen in the amide linker contributes to overall binding by forming a hydrogen bond to Arg186. The HN group in the amide linker does not participate in any significant interactions. The pyridine ring has important contribution due to its hydrogen bond to Ser159 and possible π–π interaction with Phe161. However, it is still underexploited. In the vicinity of the pyridine ring are the carboxamide groups of Asn138 and Gln162, which could provide additional hydrogen bonds.

NMR results indicate that compound **1** interacts only with *N*-terminal and central domain. Our recently published study revealed that MurD domains' flexibility may negatively affect the binding of sulfonamide inhibitors [8,9]. Slight opening/closing movement between *N* and *C*-terminal domains was observed which tend to weaken ligand–protein interactions. In this study, the overlap of the most "closed" and most "open" conformation of MurD reveals that this domain movement does not significantly affect binding of compound **1** (Fig. 10). Thus, the inhibitors that mimic UMA substrate and target only the binding site located in the *N*-terminal and central domain may possess certain advantages.

Compound **1** dose not interact with the *C*-terminal domain. Its scaffold has two novel binding elements which makes its binding mode different from other MurD inhibitors (Figs. 11 and 12). The pyridine ring occupies a place in central binding domain, which was so far not occupied by other MurD inhibitors. The 2-oxoindolinylidene ring occupies larger volume in the uracil binding pocket in comparison to other inhibitors, therefore, producing more interactions with the protein residues.

3. Conclusion

A 2-oxoindolinylidene derivative (compound **1**), a new structure scaffold, was discovered and demonstrated to inhibit MurD enzyme inhibition. The compound **1** also possesses weak antibacterial activity against a set of standard bacterial strains in contrast to most MurD inhibitors we reported previously. We expect that much stronger inhibition will be realized by the structure modification of

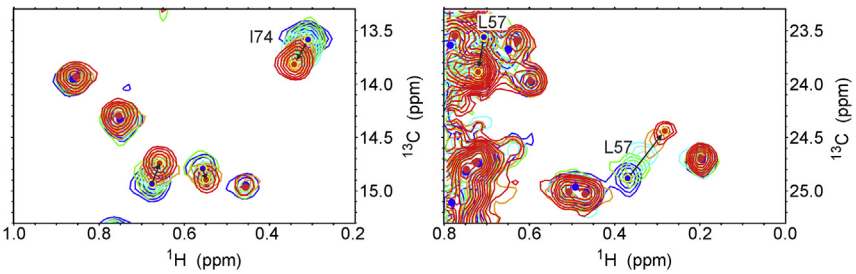

Fig. 6. The parts of the ^{1}H/^{13}C-HSQC spectrum with the numbering of the resonances indicating interaction of compound **1** with the uracil binding pocket. Different colors indicate different ligand:protein molar ratios: blue no ligand, green 0.5:1, cyan 1:1, orange 2:1, red 5:1. Peak positions of the MurD without ligand and with ligand at final ratio are marked with blue and red dots respectively. Signals that are indicative for the binding in the uracil binding pocket are highlighted with yellow outlines. (For interpretation of the references to color in this figure legend, the reader is referred to the web version of this article.)

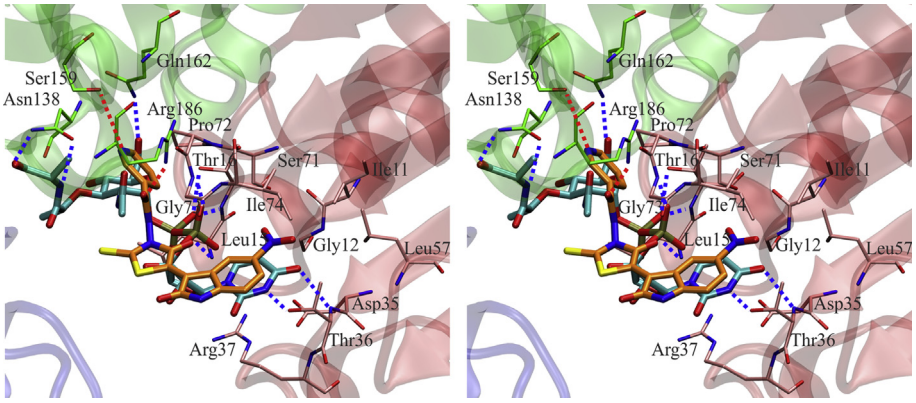

Fig. 7. Stereoview of a snapshot from the MD trajectory showing the binding mode of compound **1** (orange) in the MurD binding site (MD simulation started from structure 3). The location of UMA (cyan) in the binding site is overlaid for comparison [2]. *N*-terminal, central and *C*-terminal domains are represented in red, green and blue respectively. (For interpretation of the references to color in this figure legend, the reader is referred to the web version of this article.)

the new scaffold as pointed out below by our NMR and molecular modeling study.

The NMR and MD of new MurD inhibitor revealed a different mode of binding compared to the naphthalene-*N*-sulfonyl-D-glutamic acid derivatives. The pattern of the CSP of MurD methyl groups upon binding of compound **1** clearly indicates that it is located in the UMA binding site and interacts only with the *N*-terminal and central MurD domains. The 2-oxoindolinylidene ring is located in the uracil binding site, while the 4-oxo-2-thioxo-1,3-thiazolidine ring and the pyridine ring are close to the part of the binding site occupied by the UMA phosphate groups and *N*-acetylmuramic acid ring respectively. Although compound **1** exhibits much less hydrogen bonding than UMA, it is firmly anchored in the proposed binding mode during the MD simulation, thus demonstrating the importance of hydrophobic interactions in the uracil binding pocket. The binding of the new inhibitor is not affected by the protein domain motions, because it does not interact with the *C*-terminal domain.

We got good insight into the interaction profile of the new structure scaffold of compound **1** and found that the rigid double bond between 2-oxoindolinylidene ring and 4-oxo-2-thioxo-1,3-thiazolidine ring is unfavorable and should be released. Additional hydrophobic contacts would contribute favorably. Spatial distribution of polar and hydrophobic interactions exerted by the structure fragments gives us a strong starting point for the *de novo* design of new ligands that could achieve higher binding affinities. Since the uracil-binding pockets of the Mur ligases C to F active sites are the most highly conserved and the MurC-F substrates share identical UDP/MurNAc substrate moieties, the structural characteristics of new inhibitor and mode of interaction should provide more rational search and design of a new generation of specific bacterial cell wall inhibitors.

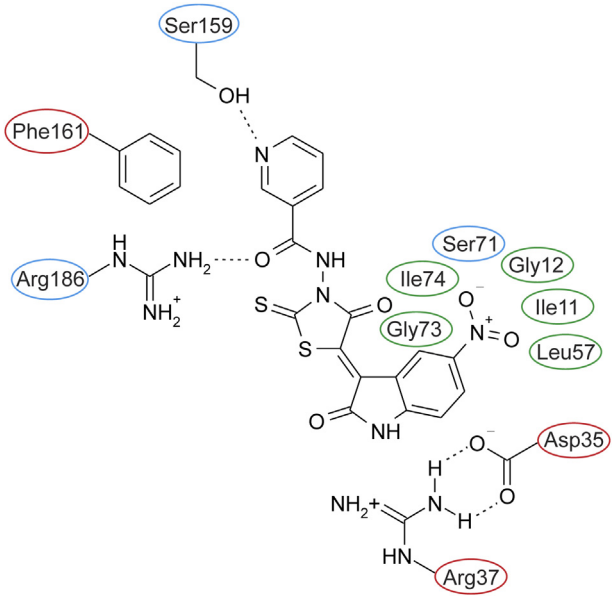

Fig. 8. Schematic presentation of the binding interactions of compound **1** with the MurD residues. Residues contributing to electrostatic, hydrophobic and π–π interactions are colored in blue, green and red respectively. (For interpretation of the references to color in this figure legend, the reader is referred to the web version of this article.)

4. Experimental procedures

4.1. Materials

Compound **1** was purchased from the commercially available AsinexGold compound collection (www.asinex.com). UMA was purchased from University of Warwick. AMP-PCP was provided from Sigma. Naphthalene-*N*-sulfonyl-D-Glu derivatives compound **2** and compound **3** were prepared by Humljan et al. [6] and Sosič et al. [7]. Elemental analysis was used to determine the purity of compounds, which is ≥95%.

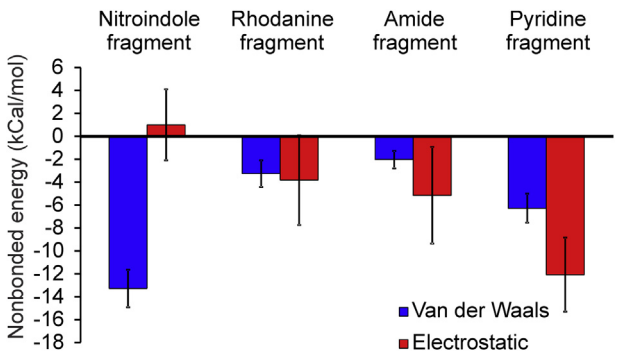

Fig. 9. Nonbonded energy contributions during MD simulation of the compound **1** – MurD complex (MD simulation started from structure 3). Average energies and their standard deviations over the trajectory are shown.

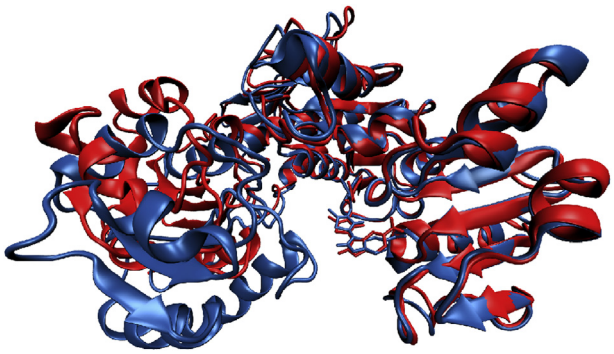

Fig. 10. Snapshots from MD trajectory showing most "closed" (blue) and most "open" (red) conformation of MurD in complex with compound **1**. (For interpretation of the references to color in this figure legend, the reader is referred to the web version of this article.)

4.2. Steady-state enzyme kinetic analysis

The formation of orthophosphate generated during the MurD catalyzed reaction was followed spectrophotometrically in a microplate reader using slightly modified malachite green assay described before [20]. All reactions were run in a final volume of 50 μL containing 50 mM Hepes, pH 8.0, 3.25 mM $MgCl_2$, 10 mM $(NH_4)_2SO_4$, 0.005% Triton X-114, 80 μM UMA, 100 μM D-Glu, 400 μM ATP and 5% DMSO with purified MurD from *Escherichia coli*, diluted with 50 mM Hepes, pH 8.0, 1 mM dithiothreitol, as described previously [5]. The reaction mixture was incubated at 37 °C for 15 min and then quenched with 100 μL of Biomol Green™ reagent (Enzo Life Sciences). Absorbance at 650 nm was measured after 5 min. A blank sample, which contained assay buffer, instead of the enzyme, was used to eliminate the effects of the background absorbance.

The apparent K_M values for each substrate were determined using variable concentration of one substrate (ATP: 20–400 μM, D-Glu: 15–120 μM, UMA: 2–80 μM) at the constant concentrations of the other two substrates (ATP: 400 μM, D-Glu: 100 μM, UMA: 80 μM). Data were collected in duplicate.

The mode of inhibition was determined under the same conditions in duplicates; different concentrations of one substrate and fixed concentrations of the other two with inhibitor concentrations from 0 to 500 μM. Initial velocity data were fitted to competitive, noncompetitive, uncompetitive and mixed-type inhibition models using GraphPad Prism 5.04 software (San Diego, CA). The best fit with the highest R^2, the lowest standard error and the narrowest 95% confidence interval in each parameter were taken.

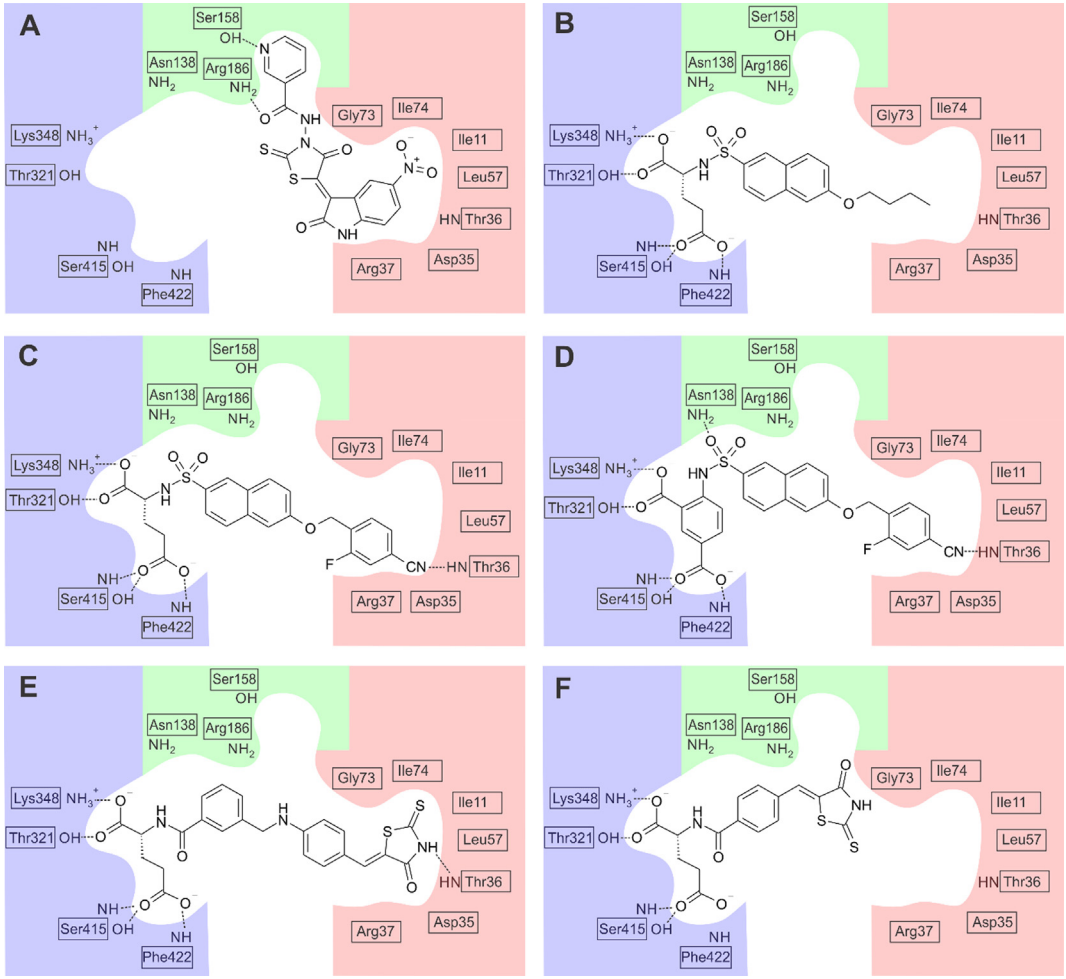

Fig. 11. Schematic comparison of binding modes of different MurD inhibitors: (A) Compound **1**, (B) Compound **2** (First generation alkyloxy substituted sulfonamide inhibitor), (C) Compound **3** (First generation arylalkyloxy substituted sulfonamide inhibitor), (D) Second generation sulfonamide inhibitor with rigid D-Glu mimetic, (E) 5-benzylidenerhodanine inhibitor, (F) 5-Thioxothiazolidoine-4-one inhibitor. *N*-terminal, central and *C*-terminal domains regions are represented in red, green and blue respectively. (For interpretation of the references to color in this figure legend, the reader is referred to the web version of this article.)

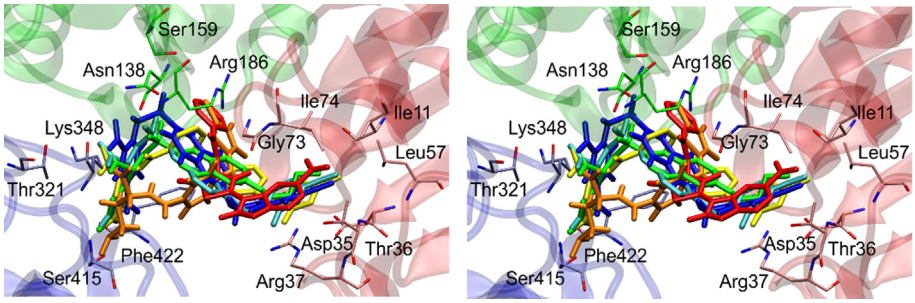

Fig. 12. Stereoview of a superposition of different MurD inhibitors in the MurD binding site: Compound **1** (red), Compound **2** (green), Compound **3** (cyan), Second generation sulfonamide inhibitor with rigid D-Glu mimetic (blue), 5-benzylidenerhodanine inhibitor (yellow), 5-Thioxothiazolidoine-4-one inhibitor (orange). *N*-terminal, central and *C*-terminal domains are represented in red, green and blue respectively. (For interpretation of the references to color in this figure legend, the reader is referred to the web version of this article.)

4.3. Antibacterial activity

Minimal inhibitory concentrations (MICs) of compound **1** were determined by broth microdilution method against gram-negative strains *E. coli* (ATCC 25922), *E. coli* (ATCC 35218), *H. influenzae* (ATCC 49247), *H. influenzae* (Lek 93) and gram-positive strains *Streptococcus aureus* (ATCC 25923), *Streptococcus pneumoniae* (ATCC 49619), *Streptococcus pyogenes* (ATCC 19615) and *E. faecalis* (ATCC 29212). The MIC was taken as the lowest concentration that prevented the growth of bacteria in a well. The MIC determination was performed in accordance with the standard reference recommendations of the CLSI [21].

4.4. Isolation and purification of unlabeled and $^{15}N/^{13}C$ selectively labeled E. coli MurD enzyme

Recombinant unlabeled *E. coli* MurD ligase was overexpressed and purified using the 6 × His-tag system as reported earlier [5,8]. The $^{15}N/^{13}C$ methyl (Ile (δ1), Val and Leu) selectively labeled protein was overexpressed according to a modified procedure previously described [22] and purified according to a procedure previously used in our laboratory for unlabeled MurD enzyme [8]. *E. coli* BL21(DE3)pLysS cells, freshly transformed with pABD16/MurD vector, were grown overnight at 37 °C in 10 mL of LB (Sigma) rich growth medium containing ampicillin (Sigma) (100 mg/L). Cells were spun down, resuspended in 50 mL of M9 minimal medium containing 6.5 g/L Na_2HPO_4, 3 g/L KH_2PO_4, 0.5 g/L NaCl, 1 g/L NH_4Cl, 3 g/L D-glucose, 120 mg/L $MgSO_4$, 11 mg/L $CaCl_2$, 10 mg/L thiamine, 10 mg/L biotin, 100 mg/L ampicillin and grown to reach $A_{600\ nm}$ of 0.1. Cells were spun down and resuspended in 200 mL of ^{15}N labeled M9 medium. At $A_{600\ nm}$ of about 0.5, the cells were transferred to 2 flasks containing 400 mL of ^{15}N labeled M9 medium. At $A_{600\ nm}$ of 0.25, α-ketobutyrate (methyl ^{13}C, 99%) (Cambridge Isotope Laboratories) and α-ketoisovalerate (dimethyl $^{13}C_2$, 99%) (Cambridge Isotope Laboratories) solutions were added at a final concentration of 70 mg/L and 120 mg/L respectively. Growth was continued for one hour. Expression was induced with β-D-thiogalactopyranoside (IPTG) (Inalco) at a final concentration of 1 mM. Growth was continued for 8 h. The cells were harvested and resuspended in buffer containing 20 mM potassium phosphate, 1 mM dithiothreitol (DTT, Sigma), pH 7.2. The cells were lysed by ultrasound sonication. The suspension was centrifuged and the pellet was discarded. Pre-equilibrated Ni^{2+}-nitrilotriacetate-agarose resin (Ni^{2+}-NTA) (Qiagen) was added to the supernatant and incubated on a multi-function tube rotator for one hour. The suspension was centrifuged to recover the resin. The protein was eluted with increasing concentrations of imidazole (Sigma) (20, 40, 100 mM) in buffer containing 50 mM potassium phosphate (Sigma), 200 mM KCl and 1 mM dithiothreitol (Sigma), pH 8.0.

Fractions containing protein were collected and checked using SDS-PAGE electrophoresis. Fractions containing MurD protein with the purity greater than 95% were joined and concentrated using an Amicon Ultra 10K NMWL concentrator. Samples were dialyzed against buffer containing 20 mM HEPES, 7 mM $(NH_4)_2SO_4$, 3.5 mM $MgCl_2$, 0.3 mM DTT (all Sigma), pH 7.2. Protein concentration was determined by measuring A_{280} on a Nanodrop ND-1000 spectrophotometer. Glycerol (1,1,2,3,3-D_5, 99%, CIL) was added to the protein solution (10% v/v), and the solution was frozen at −24 °C.

4.5. Nuclear magnetic resonance

The NMR spectra were recorded at 25 °C on a Varian DirectDrive 800 MHz spectrometer equipped with a Cryoprobe. The pulse sequences provided in the Varian BioPack library of pulse programs were used. Samples were prepared in 90%H_2O/10%DMSO-d_6 buffer containing 20 mM HEPES, 7 mM $(NH_4)_2SO_4$, 3.5 mM $MgCl_2$, 0.3 mM DTT and 2 mM β,γ-Methyleneadenosine 5′-triphosphate (AMP-PCP), pH 7.2. The concentration of MurD selectively labeled with ^{13}C at the methyl groups of Ile (δ1 only), Val and Leu was 0.07 mM. The protein was titrated using the ligands (**1**, **2**, **3**, UMA, and D-Glu) in MurD:ligand molar ratios of 0.5, 1, 2, 5 and 10. Due to lower solubility, ligand **1** could only be added up to a MurD:ligand molar ratio of 1:5.

The $^1H/^{13}C$-HSQC [23] spectra were acquired with 1024 data points in t_2, 32 scans, 64 complex points in t_1 and a relaxation delay of 1 s. The ^1H and ^{13}C sweep widths were 9470 and 3340 Hz respectively. Spectra were processed with NMRPipe software [24] and analyzed with Sparky software [25]. Spectra were zero-filled twice and apodized with a squared sine bell function shifted by π/2 in both dimensions, using a linear prediction of the data in the incremented dimension.

The combined $^1H/^{13}C$ CSP (Δδ) were calculated from ^1H and ^{13}C CSP using the equation: $\Delta\delta = ((\Delta\delta^1H)^2 + (0.252 \times \Delta\delta^{13}C)^2)^{1/2}$ [26]. The K_D values were determined by nonlinear least squares fitting of CSP (Δδ) versus ligand concentration (L) according to the equation: $\Delta\delta = \Delta\delta_{max}([L]_T + ([P]_T + K_D - (([L]_T + ([P]_T + K_D)^2 - 4[L]_T([P]_T)^{1/2})/(2[P]_T)$, where $[L]_T$ and $[P]_T$ pertain to the total ligand and protein concentration respectively; $\Delta\delta_{max}$ is the CSP at saturation [26].

STD ligand epitope mapping experiments were performed at 800 MHz with an 8389 Hz spectral width, 16,384 data points, a saturation time of 350 ms, a relaxation delay of 11.35 s and 3000 scans. Spectra were recorded at an enzyme:ligand ratio of 1:100. Selective saturation was achieved by a train of 50 ms long Gauss-shaped pulses separated by a 1 ms delay. Water was suppressed via excitation sculpting. The on-resonance selective

saturation of the enzyme was applied at 0.21 ppm. Off-resonance irradiation was applied at 30 ppm for the reference spectrum. Subtraction of on- and off-resonance spectra was performed internally via phase cycling. Spectra were zero-filled twice and apodized by an exponential line broadening function of 1 Hz.

4.6. Molecular modeling calculations

Calculations were performed on GNU/Linux-based personal computers at the National Institute of Chemistry in Ljubljana, utilizing the CHARMM molecular modeling suite [27–29], developmental version 36a1. MurD protein coordinates were obtained from the Protein Data Bank PDB entry 2JFF. Force field parameters were obtained from the CHARMM parameter and topology files (version 27) for proteins [28,29] and from the CHARMM General Force Field (CGenFF) parameter and topology files for drug-like molecules [30]. Missing dihedral angle parameters were optimized using a Gaussian 09 program [31]. CHARMM dihedral angle parameters were adjusted to obtain an energy profile comparable to that calculated in Gaussian 09. The charges on the oxygen and sulfur atoms on the 4-oxo-2-thioxo-1,3-thiazolidine fragment were optimized by adding water molecules and by calculating the interaction energy using Gaussian 09. CHARMM parameters were adjusted to obtain the same interaction energy as the energy calculated *ab initio* in Gaussian 09. The compounds alone were subjected to energy minimization using the Adopted Basis Newton–Raphson method and then hydrated by immersion into a cubic box (86 Å × 86 Å × 86 Å) of water molecules. Deletion of water molecules overlapping with the protein resulted in a system with approximately 20,000 TIP3 water molecules. The entire system was again subjected to energy minimization using the Adopted Basis Newton–Raphson method. MD simulations were run at 1 fs time steps for 2 ns. A CPT ensemble was used in all calculations, with the pressure at 1 bar and temperature at 300 K. Electrostatic interactions were computed using the Ewald particle-mesh method. The system was equilibrated after 100 ps of MD simulation, therefore the first 100 ps of MD trajectory were not considered in the analysis.

Acknowledgment

This work was supported by the Ministry of Higher Education, Science and Technology of Slovenia (Grant No. J1-0317-0104-08 and P1-0010), Lek Pharmaceuticals d.d., EN-FIST Centre of Excellence and the European Union FP6 Integrated Project EUR-INTAFAR (Project No. LSHM-CT-2004-512138) under the thematic priority Life Sciences, Genomics and Biotechnology for Health. We are very grateful to Prof. Dr. Stanislav Gobec, Faculty of Pharmacy, University of Ljubljana, for his support in carrying out our project.

Appendix A. Supplementary data

Supplementary data related to this article can be found at http://dx.doi.org/10.1016/j.ejmech.2014.06.021.

References

[1] J.A. Bertrand, G. Auger, E. Fanchon, L. Martin, D. Blanot, J. van Heijenoort, O. Dideberg, Crystal structure of UDP-*N*-acetylmuramoyl-L-alanine: D-glutamate ligase from *Escherichia coli*, EMBO J. 16 (1997) 3416–3425.
[2] J.A. Bertrand, G. Auger, L. Martin, E. Fanchon, D. Blanot, D. Le Beller, J. van Heijenoort, O. Dideberg, Determination of the MurD mechanism through crystallographic analysis of enzyme complexes, J. Mol. Biol. 289 (1999) 579–590.
[3] M.E. Tanner, S. Vaganay, J. van Heijenoort, D. Blanot, Phosphinate inhibitors of the D-glutamic acid-adding enzyme of peptidoglycan biosynthesis, J. Org. Chem. 61 (1996) 1756–1760.
[4] L.D. Gegnas, S.T. Waddell, R.M. Chabin, S. Reddy, K.K. Wong, Inhibitors of the bacterial cell wall biosynthesis enzyme Mur D, Bioorg. Med. Chem. Lett. 8 (1998) 1643–1648.
[5] M. Kotnik, J. Humljan, C. Contreras-Martel, M. Oblak, K. Kristan, M. Hervé, D. Blanot, U. Urleb, S. Gobec, A. Dessen, T. Šolmajer, Structural and functional characterization of enantiomeric glutamic acid derivatives as potential transition state analogue inhibitors of MurD ligase, J. Mol. Biol. 370 (2007) 107–115.
[6] J. Humljan, M. Kotnik, C. Contreras-Martel, D. Blanot, U. Urleb, A. Dessen, T. Šolmajer, S. Gobec, Novel naphthalene-*N*-sulfonyl-D-glutamic acid derivatives as inhibitors of MurD, a key peptidoglycan biosynthesis enzyme, J. Med. Chem. 51 (2008) 7486–7494.
[7] I. Sosič, H. Barreteau, M. Simčič, R. Šink, J. Cesar, A. Zega, S. Golič Grdadolnik, C. Contreras-Martel, A. Dessen, A. Amoroso, B. Joris, D. Blanot, S. Gobec, Second-generation sulfonamide inhibitors of D-glutamic acid-adding enzyme: activity optimisation with conformationally rigid analogues of D-glutamic acid, Eur. J. Med. Chem. 46 (2011) 2880–2894.
[8] M. Simčič, M. Hodošček, J. Humljan, K. Kristan, U. Urleb, D. Kocjan, S. Golič Grdadolnik, NMR and molecular dynamics study of the binding mode of naphthalene-*N*-sulfonyl-D-glutamic acid derivatives: novel MurD ligase inhibitors, J. Med. Chem. 52 (2009) 2899–2908.
[9] M. Simčič, I. Sosič, M. Hodošček, H. Barreteau, D. Blanot, S. Gobec, S.G. Grdadolnik, The binding mode of second-generation sulfonamide inhibitors of MurD: clues for rational design of potent MurD inhibitors, PLoS ONE 7 (2012) e52817.
[10] N. Zidar, T. Tomašić, R. Šink, V. Rupnik, A. Kovač, S. Turk, D. Patin, D. Blanot, C. Contreras Martel, A. Dessen, M. Mueller Premru, A. Zega, S. Gobec, L. Peterlin Mašič, D. Kikelj, Discovery of novel 5-benzylidenerhodanine and 5-benzylidenethiazolidine-2,4-dione inhibitors of MurD ligase, J. Med. Chem. 53 (2010) 6584–6594.
[11] N. Zidar, T. Tomašić, R. Šink, A. Kovač, D. Patin, D. Blanot, C. Contreras-Martel, A. Dessen, M.M. Premru, A. Zega, S. Gobec, L.P. Mašič, D. Kikelj, New 5-benzylidenethiazolidin-4-one inhibitors of bacterial MurD ligase: design, synthesis, crystal structures, and biological evaluation, Eur. J. Med. Chem. 46 (2011) 5512–5523.
[12] T. Tomašić, N. Zidar, R. Šink, A. Kovac, D. Blanot, C. Contreras-Martel, A. Dessen, M. Müller-Premru, A. Zega, S. Gobec, D. Kikelj, L. Peterlin Maši&ccaron, Structure-based design of a new series of D-glutamic acid-based inhibitors of bacterial UDP-*N*-acetylmuramoyl-L-alanine:D-glutamate ligase (MurD), J. Med. Chem. 54 (2011) 4600–4610.
[13] M. Kotnik, P.S. Anderluh, A. Prezelj, Development of novel inhibitors targeting intracellular steps of peptidoglycan biosynthesis, Curr. Pharm. Des. 13 (2007) 2283–2309.
[14] T. Tomašić, N. Zidar, A. Kovač, S. Turk, M. Simčič, D. Blanot, M. Müller-Premru, M. Filipič, S.G. Grdadolnik, A. Zega, M. Anderluh, S. Gobec, D. Kikelj, L. Peterlin Mašič, 5-benzylidenethiazolidin-4-ones as multitarget inhibitors of bacterial Mur ligases, ChemMedChem 5 (2010) 286–295.
[15] P.J. Hajduk, D.J. Augeri, J. Mack, R. Mendoza, J. Yang, S.F. Betz, S.W. Fesik, NMR-based screening of proteins containing 13C-labeled methyl groups, J. Am. Chem. Soc. 122 (2000) 7898–7904.
[16] K. Kristan, M. Kotnik, M. Oblak, U. Urleb, New high-throughput fluorimetric assay for discovering inhibitors of UDP-*N*-acetylmuramyl-L-alanine: D-glutamate (MurD) ligase, J. Biomol. Screen. 14 (2009) 412–418.
[17] G.C.K. Roberts, The determination of equilibrium dissociation constants of protein-ligand complexes by NMR, in: O. Zerbe (Ed.), BioNMR in Drug Research, Wiley-VCH, 2003, pp. 309–319.
[18] T. Tomašić, A. Kovač, M. Simčič, D. Blanot, S. Golič Grdadolnik, S. Gobec, D. Kikelj, L. Peterlin Mašič, Novel 2-Thioxothiazolidin-4-one inhibitors of bacterial MurD ligase targeting D-Glu- and diphosphate-binding sites, Eur. J. Med. Chem. 46 (2011) 3964–3975.
[19] C.S. Rye, J.B. Baell, Phosphate isosteres in medicinal chemistry, Curr. Med. Chem. 12 (2005) 3127–3141.
[20] P.A. Lanzetta, L.J. Alvarez, P.S. Reinach, O.A. Candia, An improved assay for nanomole amounts of inorganic phosphate, Anal. Biochem. 100 (1979) 95–97.
[21] M.A. Wikler, Methods for Dilution Antimicrobial Susceptibility Tests for Bacteria That Grow Aerobically: Approved Standard M7–A7, seventh ed., Clinical and Laboratory Standards Institute, Wayne, PA, 2006.
[22] V. Tugarinov, V. Kanelis, L.E. Kay, Isotope labeling strategies for the study of high-molecular-weight proteins by solution NMR spectroscopy, Nat. Protoc. 1 (2006) 749–754.
[23] L. Kay, P. Keifer, T. Saarinen, Pure absorption gradient enhanced heteronuclear single quantum correlation spectroscopy with improved sensitivity, J. Am. Chem. Soc. 114 (1992) 10663–10665.
[24] F. Delaglio, S. Grzesiek, G.W. Vuister, G. Zhu, J. Pfeifer, A. Bax, NMRPipe: a multidimensional spectral processing system based on UNIX pipes, J. Biomol. NMR 6 (1995) 277–293.
[25] T.D. Goddard, D.G. Kneller. SPARKY 3. University of California, San Francisco.
[26] J. Cavanagh, W.J. Fairbrother, A.G. Palmer, M. Rance, N.J. Skelton, Protein NMR Spectroscopy: Principles and Practice, second ed., Academic Press, San Diego, 2007.
[27] B.R. Brooks, R.E. Bruccoleri, B.D. Olafson, D.J. States, S. Swaminathan, M. Karplus, CHARMM: a program for macromolecular energy, minimization, and dynamics calculations, J. Comput. Chem. 4 (1983) 187–217.
[28] A.D. MacKerell, D. Bashford, Bellott, R.L. Dunbrack, J.D. Evanseck, M.J. Field, S. Fischer, J. Gao, H. Guo, S. Ha, D. Joseph-McCarthy, L. Kuchnir, K. Kuczera,

F.T.K. Lau, C. Mattos, S. Michnick, T. Ngo, D.T. Nguyen, B. Prodhom, W.E. Reiher, B. Roux, M. Schlenkrich, J.C. Smith, R. Stote, J. Straub, M. Watanabe, J. Wiorkiewicz-Kuczera, D. Yin, M. Karplus, All-atom empirical potential for molecular modeling and dynamics studies of proteins, J. Phys. Chem. B 102 (1998) 3586–3616.

[29] A.D. Mackerell, M. Feig, C.L. Brooks, Extending the treatment of backbone energetics in protein force fields: limitations of gas-phase quantum mechanics in reproducing protein conformational distributions in molecular dynamics simulations, J. Comput. Chem. 25 (2004) 1400–1415.

[30] K. Vanommeslaeghe, E. Hatcher, C. Acharya, S. Kundu, S. Zhong, J. Shim, E. Darian, O. Guvench, P. Lopes, I. Vorobyov, J.A.D. Mackerell, CHARMM general force field: a force field for drug-like molecules compatible with the CHARMM all-atom additive biological force fields, J. Comput. Chem. 31 (2009) 671–690.

[31] M.J. Frisch, G.W. Trucks, H.B. Schlegel, G.E. Scuseria, M.A. Robb, J.R. Cheeseman, G. Scalmani, V. Barone, B. Mennucci, G.A. Petersson, H. Nakatsuji, M. Caricato, X. Li, H.P. Hratchian, A.F. Izmaylov, J. Bloino, G. Zheng, J.L. Sonnenberg, M. Hada, M. Ehara, K. Toyota, R. Fukuda, J. Hasegawa, M. Ishida, T. Nakajima, Y. Honda, O. Kitao, H. Nakai, T. Vreven, J.A. Montgomery, J.E. Peralta, F. Ogliaro, M. Bearpark, J.J. Heyd, E. Brothers, K.N. Kudin, V.N. Staroverov, R. Kobayashi, J. Normand, K. Raghavachari, A. Rendell, J.C. Burant, S.S. Iyengar, J. Tomasi, M. Cossi, N. Rega, J.M. Millam, M. Klene, J.E. Knox, J.B. Cross, V. Bakken, C. Adamo, J. Jaramillo, R. Gomperts, R.E. Stratmann, O. Yazyev, A.J. Austin, R. Cammi, C. Pomelli, J.W. Ochterski, R.L. Martin, K. Morokuma, V.G. Zakrzewski, G.A. Voth, P. Salvador, J.J. Dannenberg, S. Dapprich, A.D. Daniels, Ö. Farkas, J.B. Foresman, J.V. Ortiz, J. Cioslowski, D.J. Fox, Gaussian 09, Revision A.02, 2009. Wallingford CT.